Source-Receptor Relationships Between Precursor Emissions and O_3 and $PM_{2.5}$ Air Pollution Impacts

Kirk R. Baker[*],
U.S. Environmental Protection Agency, Research Triangle Park, North Carolina, 27709, USA

Heather Simon,
U.S. Environmental Protection Agency, Research Triangle Park, North Carolina, 27709, USA

Barron Henderson,
U.S. Environmental Protection Agency, Research Triangle Park, North Carolina, 27709, USA

Colby Tucker,
U.S. Environmental Protection Agency, Washington, DC, 20460, USA

David Cooley,
Abt Associates, Durham, NC, 27703, USA

Emma Zinsmeister
U.S. Environmental Protection Agency, Washington, DC, 20460, USA

Abstract

Reduced complexity tools that provide a representation of both primarily emitted particulate matter with an aerodynamic diameter less than 2.5 microns ($PM_{2.5}$), secondarily formed $PM_{2.5}$, and ozone (O_3) allow for a quick assessment of many iterations of pollution control scenarios. Here, a new reduced complexity tool, Pattern Constructed Air Pollution Surfaces (PCAPS), that estimates annual average $PM_{2.5}$ and seasonal average maximum daily average 8-hr (MDA8) O_3 for any source location in the United States is described and evaluated. Typically reduced complexity tools are not evaluated for skill in predicting change in air pollution by comparison with emission changes predicted by more sophisticated modeling systems. Here, PCAPS was compared against multiple types of emission control scenarios predicted with state-of-the-science photochemical grid models to provide confidence that the model is realistically capturing the change in air pollution due to changing emissions. PCAPS was also applied with all anthropogenic emissions sources for multiple retrospective years to predict $PM_{2.5}$ chemical components for comparison against routine surface measurements. PCAPS predicted similar magnitudes and regional variation in spatial gradients of measured chemical components of $PM_{2.5}$. Model

[*]corresponding author: baker.kirk@epa.gov.

performance for capturing ambient measurements was consistent with other reduced complexity tools. PCAPS also did well at capturing the magnitude and spatial features of changes predicted by photochemical transport models for multiple emissions scenarios for both O_3 and $PM_{2.5}$. PCAPS is a flexible tool that provides source-receptor relationships using patterns of air quality gradients from a training dataset of generic modeled sources to create interpolated air pollution gradients at new locations not part of the training database. The flexibility provided for both sources and receptors make this tool ideal for integration into larger frameworks that provide emissions changes and need estimates of air quality to inform downstream analytics, which often includes an estimate of monetized health effects.

Graphical Abstract
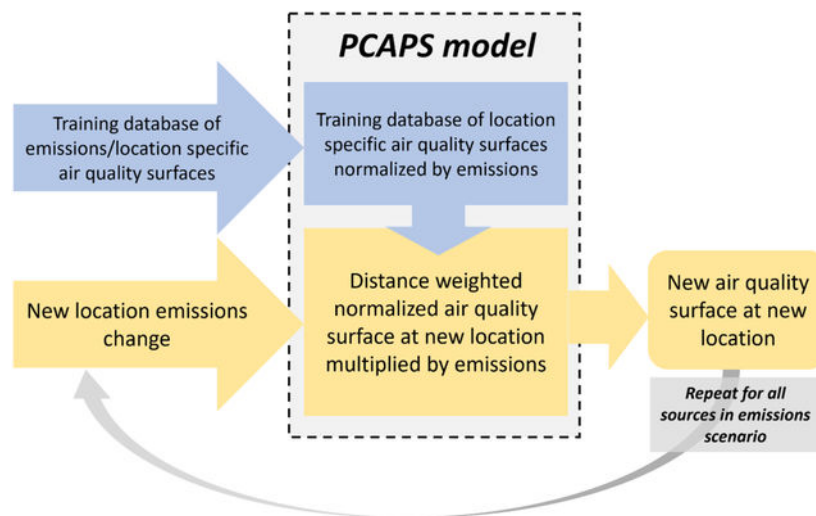
Keywords

$PM_{2.5}$; O_3; photochemical model; PCAPS; COBRA

INTRODUCTION

Ambient ozone (O_3) and particulate matter with aerodynamic diameter less than 2.5 microns ($PM_{2.5}$) both negatively impact human health[1–3]. Both pollutants are regulated by the United States Environmental Protection Agency (U.S. EPA) with National Ambient Air Quality Standards (NAAQS) (85 FR 87256 and 85 FR 82684). Many areas in the U.S. have historically been unable to meet these standards. Sophisticated air quality models that represent complex atmospheric processes (like complex gas phase chemistry) are often used to provide a quantitative estimate of the change in O_3 and $PM_{2.5}$ based on changes in emissions that reflect emission control plans intended to improve air quality in areas not compliant with the NAAQS. Photochemical grid models have also been used to quantify the impacts on air quality due to planned implementation of alternative energy strategies or changes in human activity to understand population health impacts regardless of NAAQS attainment status[4, 5]. In addition, there are a variety of reduced form tools with a range of capabilities and limitations intended to provide a much faster solution.

The application of photochemical grid models requires specialized knowledge and can be resource intensive especially for assessments that include a multitude of simulations or those with simulations covering a large area or time period. Numerous tools have been developed that provide a simplified representation of emissions, dispersion, and chemical processes to quickly provide an estimate of air quality change and human health impacts to avoid the costs associated with photochemical grid model application[6]. Some of these tools were based on a climatological dispersion model applied at the continental scale with a simplified representation of chemical transformation[7, 8] and some based on air quality impacts predicted by a photochemical transport model[9–13]. These reduced complexity tools have been used extensively to provide an estimate of $PM_{2.5}$ air quality and related monetized health impact {Buonocore, 2021 #39;Chan, 2018 #32;Goodkind, 2019 #29;Luo, 2022 #33;Strasert, 2019 #28;Thind, 2022 #34} but few provide an estimate of O_3 air quality impacts[11, 13]. Fewer still provide a quantitative evaluation against air quality changes due to changing emissions predicted by a more sophisticated modeling system (such as a photochemical grid model), which is the fundamental purpose of these tools[11].

Here, a new reduced complexity tool is described that creates source-receptor relationships using patterns of air pollution gradients estimated with a photochemical transport model for generic sources placed in a range of different chemical and physical environments in the United States. Model predicted air quality for these generic sources (the training dataset) were extrapolated to areas not part of the training dataset to provide representation of source-receptor combinations for all areas in the United States. This new model is called Pattern Constructed Air Pollution Surfaces (PCAPS) version 1.0. PCAPS provides an estimate of annual average $PM_{2.5}$ sulfate ion, $PM_{2.5}$ nitrate ion, primarily emitted $PM_{2.5}$, primarily emitted coarse fraction PM, and seasonal average maximum daily average 8-hr (MDA8) O_3 that results from a change in precursor emissions.

PCAPS utilizes 12 km meteorology which is comparable to some reduced complexity tools[9, 11] like the source apportionment-based air quality surfaces (SABAQS) tool[11] but finer scale than others such as the Intervention Model for Air Pollution (InMAP)[12], The Estimating Air pollution Social Impact Using Regression (EASIUR) model[10], and TM5-FAst Scenario Screening Tool (TM5-FASST)[13]. The source group scale used in PCAPS (12 km grid structure) is finer than most of these tools, some of which are much coarser with source groups being defined by states[11] or larger[13] and sometimes with limited sector representation[11]. Models using a source and receptor scale based on U.S. counties such as Air Pollution Emission Experiments and Policy analysis (APEEP)[8] and CO-Benefits Risk Assessment Health Impacts Screening and Mapping Tool (COBRA; epa.gov/cobra) have a similar scale for some parts of the eastern U.S. but much coarser representation of the western U.S. where counties can be very large and irregularly shaped.

Typically, documentation for reduced complexity tools provide methodological details and an illustrative example demonstrating the range of intended capability. Sometimes the air quality or monetized health impacts from these tools are intercompared for the same set of emissions but they have not traditionally been compared to air quality predictions estimated by a more complex modeling system like photochemical transport models. This new approach relating precursor emissions with downwind seasonal average MDA8 O_3 and

annual average PM$_{2.5}$ impacts is compared with photochemical grid model predictions of O$_3$ and PM$_{2.5}$ resulting from multiple complex emission control strategies and with other reduced complexity tools. Photochemical models treat complex meteorology, emissions, chemistry, and physical removal processes in the atmosphere and are considered the best approximation of the change in air quality due to changes in emissions[14]. The emission control scenarios used here for evaluation provide spatially varying magnitudes of precursor emissions across the United States for a ground level source sector (onroad mobile) and the electrical generating sector that releases pollutants aloft. Additional sector-specific scenarios (cement kilns, pulp and paper, and refineries) were used to understand how well the model captures spatially distinct sources.

PCAPS was also applied with total anthropogenic emissions representing multiple historical years (2007, 2011, and 2016) to estimate total speciated PM$_{2.5}$ components that were compared with ambient measurements made at routine surface monitors. This evaluation is intended to ensure the model does not provide a physically unrealistic representation of the magnitudes or spatial features of PM$_{2.5}$ chemical components. It is intended that the comparison against ambient measurements and predicted change in air quality with a photochemical transport model provide confidence in this approach and illustrate situations where further development may be needed.

METHODS

This reduced complexity tool uses a training database of air pollution surfaces (spatial pattern of air quality impacts) for generic emissions sources located in chemically and physically diverse locations in the United States. These source-specific air quality predictions were generated using the source apportionment feature of a photochemical grid model. The training dataset consists of generic surface level and tall stack (height = 90 m) sources, which are referred to here as training sources. Air quality impacts at each unique generic source location were normalized by emission rate and used to inform new source-receptor relationships at locations that were not part of the training database. PCAPS provides flexibility for defining source locations or source areas which could be defined as a single location, counties, or states and generate air quality impacts at similarly defined receptors (e.g., specific location, county, etc.).

The training dataset locations were largely based on areas with existing industrial emissions sources and not intended to provide a systematic representation of all areas of the contiguous United States (Figure S1). The approach for developing a training dataset by modeling specific sources with photochemical model source apportionment is similar to that used for other reduced complexity tools[9, 10, 15] but source placement and approach for using the source specific air pollution surfaces to represent new sources are substantively different. The training dataset was developed to support permit related program applications and not for this specific purpose but was chosen since it provided a rich dataset that would be very time and resource intensive to develop from scratch.

Training Dataset Overview

The Comprehensive Air Quality Model with Extensions (CAMx) version 7 (www.camx.com) was applied for a domain covering the contiguous U.S. with square 12 km sized grid cells for the entire year of 2011 and 2016. The photochemical model treats emissions, transport, chemical transformation, and removal through wet and dry deposition processes. The troposphere was vertically resolved with 35 layers that were thinnest nearest the surface to best resolve temporal variability in the surface mixing layer. Chemical inflow into the model domain was time and space variant extracted from a same year hemispheric scale photochemical model simulation. Meteorological inputs were generated with the Weather Research and Forecasting model[16] for the same grid specifications and time period modeled with the photochemical model. Emissions inputs included representation of anthropogenic (e.g., electrical generating units, industrial facilities, mobile sources), biogenic, and geogenic (e.g., fires and oceanic) sources[17].

Photochemical model predicted O_3 and speciated $PM_{2.5}$ were compared to measurements made as part of routine surface monitoring networks[18]. The model replication of MDA8 O_3 and speciated $PM_{2.5}$[19] was consistent with performance for other photochemical model simulations applied for the contiguous U.S. for policy and scientific assessments[4, 5].

CAMx was applied with source apportionment which tracks the contribution of predefined emission sources to model predicted primary and secondarily formed pollutants including O_3, $PM_{2.5}$, and coarse fraction particulate matter[20]. Photochemical grid model source apportionment tracks the contribution of precursor emissions through all chemical and physical processes in the model from predefined specific sources, sectors, and geographic regions[9, 10, 15, 21–27]. Source apportionment of specific facilities has been shown to compare well with source specific in-plume measurements of primary and secondary pollutants[28, 29]. The source apportionment feature was used to track generic sources added to the standard model inputs which varied by stack height and emission rate[30]. The combination of emission rate (500, 1000, or 3000 tpy), stack height (surface or 90 m release height), and location varied (Figure S1) because the original database was not intended to provide a systematic representation of these parameters over the contiguous U.S.

Reduced Complexity Model Development

The training database of generic source specific air pollution surfaces was used to develop new air pollution surfaces for sources that were not part of the original database (Figure S1). New air pollution surfaces were developed using the normalized air quality surfaces of nearby generic sources modulated to reflect the new source emission rate. A distance weighting approach was used to emphasize generic sources closest to the new source since those would be most similar in terms of chemical and physical environment.

Air quality surfaces for specific generic sources predicted with a photochemical grid model using source apportionment were averaged for the entire year for $PM_{2.5}$ and the warm season (April through September) for MDA8 O_3 and then normalized by annual emission rate. In situations where a single location was modeled with multiple emission rates the normalized surfaces were averaged. Separate normalized air quality surfaces were generated

for each location differentiated by emission release height (surface level and 90 m) and precursor for annual average $PM_{2.5}$ and seasonal average MDA8 O_3. Equation 1 shows how gridded normalized air quality surfaces (f with units of ppb for O_3 or μg/m3 for $PM_{2.5}$) where generated for each training source (t) based on air quality (C) normalized by generic source emission rate (E, tpy). The number (N) of generic sources varies based on how many different emission rates were modeled for a particular generic source location and release point (surface or aloft).

$$f_t = N^{-1} \sum_{e=1}^{N} C_{t,e} E_{t,e}^{-1}$$

Eq (1)

Multiple steps were needed to generate a new air quality surface. First, normalized air quality surfaces estimated with Equation 1 associated with training data sources within 1000 km of the new location were centered over the new location. Since far distant generic sources do not get used for the calculation, the number of training data sources used varies for each new location. Second, the normalized air quality surfaces were averaged together using a weighting function inversely proportional to the distance (distance$^{1.5}$ in km) between the training dataset source and new location to place greater emphasis on nearby sources and minimize the influence of sources further away. The form of the distance term is a general interpretation of the primary and secondary pollutant dispersion coefficient estimated using a regression equation to describe single source pollutant impacts[9]. These steps are described mathematically in Equation 2.

$$f_n = \frac{\sum_i f_{t,i} w_{t,i}}{\sum_i w_{t,i}} : i \in \text{training sites within 1000 km of } n$$

Eq (2)

$$C_n = E_n f_n$$

Eq (3)

Where f and $\mathbf{C}$ are 300 by 300 squares of grid cells (3600 × 3600 km area) and w is a weighting parameter. In this work, w is the distance of the training dataset generic source location to the new source location to the power of negative one and a half ($w_{t,I} = d_{t,n}^{-1.5}$). The distance weighting approach is intended to retain important regional characteristics related to wind patterns and air quality chemical regimes. However, highly localized features not captured by the training data set would not be realized as part of this approach.

Equation 2 estimates a gridded distance weighted normalized air quality surface for new sources not in the training dataset. Equation 3 estimates a gridded air pollution surface (units of ppb for O_3 and μg/m3 for $PM_{2.5}$) by multiplying the emission rate (E, tpy) for the new source by the gridded distance weighted normalized air quality surface estimated with Equation 2. The number of training sources varies depending on the number of training

sources within 1000 km of the new source and how many training sources were available for a particular pollutant and stack height (surface or aloft) combination. Emissions inputs to PCAPS can be gridded or using specific coordinates and outputs are gridded.

PCAPS includes an adjustment to capture the highly localized areas of urban VOC limited chemistry where NO_X emissions destroy O_3 faster than it can be produced. The training dataset includes generic sources located largely in NO_X limited areas (rural and suburban). Modeled O_3 formation regime estimated with a photochemical model for 2007 and 2016[31] was used to remove O_3 formation from NO_X emissions in areas considered NO_X saturated or transitional to better represent situations where NO_X emissions destroy O_3 faster than it is produced (Figure S2). In these situations, O_3 impacts from NO_X emissions sources were set to zero to provide a simple approach to represent areas that likely experience O_3 titration effects.

Normalized air quality relationships were developed for each grid cell to other grid cells in the 12 km modeling domain (shown in Figure 1) used for the photochemical grid model simulations. Separate normalized air quality relationships were developed for NO_X to O_3, VOC to O_3, primarily emitted $PM_{2.5}$, SO_2 to $PM_{2.5}$ sulfate ion, and NO_X to $PM_{2.5}$ nitrate ion. No relationships were developed for VOC to $PM_{2.5}$ due to the small amount of $PM_{2.5}$ mass expected from semi-volatile partitioning of gases to aerosol phase and the evolving science describing processes such as the semi-volatile nature of primary organic aerosol emissions and secondary organic aerosol enhancement in the presence of other chemicals[32, 33]. The training dataset did not include NH_3 emissions so a relationship to $PM_{2.5}$ ammonium ion could not be developed. Ambient measurements were not used to adjust modeled surfaces or normalize emissions to air quality impacts. Ambient measurements were only used for model performance evaluation to provide context about how well the model captures these measured values.

Model Response Evaluation Approach

PCAPS was evaluated by comparing predicted change in seasonal average MDA8 O_3 and annual average $PM_{2.5}$ for spatially and temporally heterogenous emission control scenarios with predictions made for those same scenarios using a photochemical grid model. The generic sources tracked with source apportionment used in the training dataset were not based on or used to inform these emission control scenarios. The emission scenarios focus on electrical generating units (EGUs), cement kilns, pulp and paper facilities, refineries, and onroad mobile sources[34]. The mobile and EGU emission control scenarios represent non-uniform changes in emissions across these sectors and in the case of the EGU scenario some facilities have increases in emissions and some have decreases (Figure S3). The pulp and paper and refinery sectors have uniform changes in emissions but represent very specific geographic locations. These complex emission control scenarios were not used to inform the development of PCAPS and only provide out-of-sample evaluation. Emission totals for each scenario are shown in Table S1. The surface level generic sources were used for the mobile emission scenario and elevated release generic sources were used for the other scenarios. For these emissions scenarios, emissions inputs and outputs were gridded to match the 12 km model domain used by the photochemical grid models.

Performance (Table S2) metrics used to compare the change in model prediction for each emission scenario between the reduced complexity model and photochemical model simulations were based on predictions made at each model land-based grid-cell cover the contiguous U.S. Performance metrics included in this assessment were mean bias (MB), normalized mean bias (NMB), fractional bias (FB), fractional error (FE), and Pearson correlation coefficient (r)[4, 5]. These metrics (shown in Table S2) were chosen to match recommendations for air quality models[5] and to facilitate comparison with other assessments.

Additional context is provided with metrics published elsewhere that compare three reduced complexity tools with photochemical model predicted components of $PM_{2.5}$ representing the year 2005[35]: EASIUR[10], APEEP[8], and InMAP[12]. Performance metrics for O_3 and $PM_{2.5}$ published for the source apportionment-based air quality surfaces (SABAQS) tool applied for multiple EGU emission control scenarios (one of which is the same as presented here) were also included[11]. Other reduced complexity tools were applied for the same emission control scenarios as PCAPS to provide additional context for strength of performance.

Application of Other Reduced Complexity Tools

A simple non-linear regression based tool that relates precursor emissions to air pollution[9] was applied to predict annual average $PM_{2.5}$ and seasonal MDA8 O_3 for these emissions control scenarios. Similar to PCAPS, this approach (Equation S1) uses photochemical grid model source apportionment predictions of air pollution from specific sources to build a more generalized relationship between emissions and downwind air pollution. This regression model approach relates emissions (β1), distance between the source and receptor (β2 and β3), and receptor air quality (β4) to generate a simple downwind pollution concentration gradient[9]. The training dataset for the nonlinear regression model was updated (presented here as NLIN2) to be consistent with the generic sources used for PCAPS. New beta coefficients were estimated for surface and aloft releases (Table S3). A spatial surface of ammonia concentrations was generated with a photochemical grid model and used to support the prediction of $PM_{2.5}$ nitrate ion (Figure S3). The NLIN2 model was applied with gridded 12 km emissions inputs and provided output for the same 12 km model domain.

The CO-Benefits Risk Assessment Health Impacts Screening and Mapping (COBRA) (epa.gov/cobra) version 4.1 tool was applied for these emission scenarios to estimate change in annual average $PM_{2.5}$. This tool does not provide an estimate of O_3 or the speciated components of $PM_{2.5}$, only total mass. The model was applied with county level emissions inputs. County level predictions were interpolated to the model domain grid specifications based on fractional county coverage in each grid cell for direct comparison with photochemical model predictions.

Ambient Measurements Evaluation Approach

Ambient measurements of major speciated components of $PM_{2.5}$ (sulfate ion, nitrate ion, elemental carbon)[18] were compared with PCAPS predictions as another type of evaluation to ensure model predictions were not physically unrealistic. For this comparison, emissions from all sources of anthropogenic pollution were input to PCAPS to provide an

estimate of annual average $PM_{2.5}$ sulfate, nitrate, and elemental carbon in each model grid cell. Emissions were based on the National Emissions Inventory (https://www.epa.gov/air-emissions-inventories/national-emissions-inventory-nei). PCAPS predictions were generated based on emissions from all sources of anthropogenic pollution representing 2007, 2011, and 2016. Ambient speciated $PM_{2.5}$ data was aggregated to annual average and compared with model predictions for 2007, 2011, and 2016. Model predictions from these retrospective years were paired in space and time (aggregated annually) with surface measurements of $PM_{2.5}$ species.

Ambient measurements were not used to adjust PCAPS model predictions. The same performance metrics (Table S2) used to compare model response were used to compare model predictions of speciated $PM_{2.5}$ with ambient data. These performance metrics were compared to other assessments using reduced complexity tools[35] to provide context for how well this tool predicts annual average speciated components of $PM_{2.5}$. This comparison against ambient measurements was done with and without an estimate of the contribution of lateral boundary inflow. The estimate of lateral boundary inflow was estimated using photochemical grid model source apportionment that was configured to specifically track this part of speciated $PM_{2.5}$[21]. Model predictions of seasonal average MDA8 O_3 could not be directly compared to ambient measurements because a non-trivial component of seasonal average MDA8 O_3 originates from sources that originate from locations outside the modeled domain and are not included in the NEI such as international anthropogenic emissions, international natural emissions, lightning and the stratosphere[21, 36]. This reduced complexity tool is based on U.S. anthropogenic emissions sources and was not designed to account for impacts from boundary inflow, biogenic, or geogenic sources.

RESULTS

Photochemical model predicted change in seasonal average MDA8 O_3 and annual average $PM_{2.5}$ for multiple complex emission scenarios[34] were used to evaluate PCAPS. Performance metrics comparing PCAPS (aloft training sources for the EGU and sector scenarios and surface level training sources for the mobile source scenario) and photochemical grid model predicted changes in seasonal average MDA8 O_3 are shown in Table 1 and for annual average $PM_{2.5}$ in Table 2.

Photochemical and PCAPS predicted change in seasonal average MDA8 O_3 and annual $PM_{2.5}$ are shown in Figures 1 and 2. Both Figures also show the difference in predicted change between the PCAPS approach and photochemical grid model. Figure 3 shows aggregated performance metrics (correlation coefficient, fractional bias, and fractional error) comparing PCAPS and photochemical model predicted change in components of annual average $PM_{2.5}$, total $PM_{2.5}$, and seasonal average MDA8 O_3. This Figure also shows performance metrics for other reduced complexity tools (COBRA, NLIN2, and SABAQS) applied for these emissions scenarios. SABAQS was applied for the EGU scenario only. Additional context is provided in Figure 3 by presenting performance metrics published in the literature for model intercomparisons[35] and other emissions scenarios not included here[11].

Predicted Changes in Seasonal Average MDA8 O_3

The PCAPS predicted change in seasonal average MDA8 O_3 compares well with photochemical model predictions (Figure 1 and Table 1): r=0.94 for the mobile scenario and r=0.92 for the EGU scenario. The spatial gradients and magnitude of seasonal MDA8 O_3 predictions using PCAPS were consistent with the photochemical grid model (Figure 1). Performance was better for the PCAPS approach compared to non-linear regression model: r=0.90 for the mobile scenario and r=0.84 for the EGU scenario (Table S4). Regional performance features were similar for NLIN2 (Figure S4) compared to PCAPS but were more prominent. PCAPS (r=0.92, FB=−16%, FE=24%) showed similar correlation to the SABAQS tool (r=0.88, FB=57%, FE=58%) applied for the same EGU emissions scenario and better fractional bias and error metrics[11].

The industrial sector emissions scenarios provide an opportunity to better understand how well PCAPS represents less ubiquitous sources. The pulp and paper sector is largely located in the southeast U.S. and refineries tend to be isolated into single facilities or small clusters[34]. PCAPS did best at capturing the change in O_3 estimated by the photochemical model for the cement kiln (r=0.92, FE=16%) and pulp and paper sectors (r=0.96, FE=21%). The model was most challenged by the refinery sector (r=0.68, FE=25%), which has the smallest emissions and is the most geographically isolated of these emissions scenarios. The NLIN2 approach had similar correlations but worse fractional error for pulp and paper (r=0.98, FE=37%) and refineries (r=0.66, FE=40%) compared to PCAPS. Both correlation and fractional error compared less favorably for the cement kiln scenario (r=0.77, FE=40%). These sector scenarios suggest that while PCAPS does well at replicating more geographically isolated scenarios (e.g., refineries scenario), inadequacies in spatial coverage of the underlying training dataset becomes more important for certain locations where generic source are sparse (Figure S1). Overall, for the 5 emissions scenarios modeled with PCAPS none exceeded 25% for fractional bias or fractional error which is better than NLIN2 (none exceeded 40%) and SABAQS (FE=58%). These performance metrics were also comparable or better than the change in predicted $PM_{2.5}$ shown here and elsewhere for similar tools predicting $PM_{2.5}$ impacts (Figure 3).

Seasonal average MDA8 O_3 was not always fully captured in urban areas with complex transitions between NO_X limited and NO_X saturated O_3 formation regimes. This limitation was sometimes evident for the surface level mobile source emission scenario but not the EGU source scenario which largely includes facilities located in NO_X limited areas outside of large urban centers. Areas known to be strongly VOC limited were much larger in 2007 compared to 2016[31] which suggests this limitation will be less important as more recent years are modeled or for years projected into the future if NO_X emissions continue to decline in urban areas.

Predicted Changes in Annual Average $PM_{2.5}$

PCAPS captures the spatial gradients in annual $PM_{2.5}$ over the contiguous U.S. predicted by the photochemical models but shows some regional scale underestimation (Figure 2). The correlation between the PCAPS predicted change in annual average $PM_{2.5}$ and the photochemical grid model was strong for both the mobile (r=0.92) and EGU (r=0.90)

scenarios and comparable to the performance shown for seasonal MDA8 O_3 impacts. PCAPS compared better to photochemical grid model predicted change in annual average $PM_{2.5}$ for both emission scenarios than two additional methods applied here (Figure 3): the nonlinear regression model (r=0.91 for the mobile scenario and r=0.84 for the EGU scenario) and the existing COBRA tool (r=0.71 for the mobile scenario and r=0.58 for the EGU scenario). The COBRA tool showed substantial regional systematic biases compared to the photochemical grid model (Figure S5, Table S5) in areas where emissions changes were largest. The NLIN2 approach showed less bias compared to the photochemical model than the COBRA tool but often overpredicted $PM_{2.5}$ impacts for the EGU scenario in areas such as the western U.S. and underpredicted $PM_{2.5}$ impacts in the upper midwest for the mobile scenario (Figure S6, Table S6). The SABAQS (r=0.94, FB=31%, FE=35%) approach had a slightly better correlation for total $PM_{2.5}$ change for the EGU scenario but worse fractional bias and error metrics than PCAPS (r=0.90, FB=−15%, FE=25%).

The comparison of photochemical model $PM_{2.5}$ with PCAPS is more complex given that the chemical constituents making up $PM_{2.5}$ can vary regionally and some forms of $PM_{2.5}$ involve more complex physical and chemical processes. The correlation between PCAPS and photochemical model predicted change in $PM_{2.5}$ sulfate ion for the EGU scenario (r=0.96) and mobile scenario (r=0.52) compare well with multiple reduced complexity tools where the correlation ranged between 0.35 to 0.58[35]. The correlation for $PM_{2.5}$ nitrate ion here (r=0.88 for the mobile scenario and 0.58 for the EGU scenario) is higher than shown for other similar tools (−0.035 to 0.054)[35]. Primary $PM_{2.5}$ (represented as elemental carbon) estimated for these scenarios (0.92 to 0.70) was comparable to those estimated elsewhere (0.73 to 0.83)[35].

Spatial plots of regional performance by $PM_{2.5}$ chemical component for each emission scenario are shown in Figures S7 to S9 (and Figures S10 to S12 for NLIN2). Performance metrics for speciated components of $PM_{2.5}$ including sulfate, nitrate, and elemental carbon are provided in Tables S7–S9. The largest chemical components of the mobile source scenario were $PM_{2.5}$ nitrate and primarily emitted $PM_{2.5}$, both of which PCAPS slightly underpredicts ($PM_{2.5}$ nitrate fractional bias = −9.7% and $PM_{2.5}$ elemental carbon bias = −18.3%) even though the spatial nature of impacts were well characterized. SO_2 emissions changes were not a substantial aspect of the mobile scenario[34], but notably impacted the normalized aggregate performance metrics for total $PM_{2.5}$ mass. In contrast for the EGU scenario, PCAPS did well at predicting both the magnitude and spatial nature of $PM_{2.5}$ sulfate ion (fractional bias = −1.3% and fractional error = 15.9%) and primarily emitted $PM_{2.5}$ (fractional bias = 15.1% and fractional error = 27.6%) compared to the photochemical model.

The industrial sector emission scenarios provide an opportunity to understand how well PCAPS captures more regionalized (pulp and paper) and localized (refineries) air pollution impacts. PCAPS tended to overestimate $PM_{2.5}$ for each of these scenarios in the eastern United States, but overall did well at capturing magnitudes and spatial patterns of emissions from each of these industrial sector emissions scenarios. Figure 3 shows how PCAPS better captures annual average $PM_{2.5}$ than the other models applied as part of this assessment and against metrics published in literature for similar types of tools. In general, PCAPS tended

to perform poorest compared to changes in air quality predicted by the photochemical grid model in regions with complex terrain with sparsely spaced emissions sources such as the western United States. The source-receptor model was most challenged replicating $PM_{2.5}$ nitrate ion impacts compared to the photochemical grid model. Poor replication of $PM_{2.5}$ nitrate ion is common and has been illustrated in other similar tools[35].

Predicted Total Ambient $PM_{2.5}$ Compared with Measurements

PCAPS (equation 3) was applied with annual total gridded SO_2, NO_X, and primary $PM_{2.5}$ emissions representing 2007, 2011, and 2016 to develop grid cell specific predictions of annual average speciated $PM_{2.5}$. These predictions were compared with measurements made at routine surface monitor networks including the Interagency Monitoring of Protected Visual Environments (IMPROVE) and the Chemical Speciation Network (CSN)[18]. Table 3 provides model performance metrics for chemical constituents of annual $PM_{2.5}$ for 2007, 2011, and 2016. Performance metrics were calculated with and without contribution from lateral boundary inflow that was estimated with photochemical grid model source apportionment[21]. Spatial plots of PCAPS predicted components of $PM_{2.5}$ with ambient data are shown in Figure 4. A comparison of model performance for predicting $PM_{2.5}$ sulfate, nitrate, and elemental carbon with other studies doing similar comparisons for reduced complexity tools is shown in Figure 5. Overall, PCAPS provided a reasonable physical representation of the magnitude and spatial distribution of $PM_{2.5}$ sulfate, nitrate, and elemental carbon. Performance metrics for PCAPS were similar to other reduced complexity tools (Figure 5).

$PM_{2.5}$ sulfate ion predicted by PCAPS compared well with the magnitude and spatial nature of ambient measurements made in 2007, 2011, and 2016 (Figure 4). $PM_{2.5}$ sulfate ion measurements and model predictions were highest in the Ohio River Valley and tend to decrease as distance from this region increases. PCAPS captured $PM_{2.5}$ nitrate ion regional gradients as the model predicted the highest levels in the upper midwest which is consistent with ambient measurements. The model underpredicted $PM_{2.5}$ nitrate ion in areas of the western U.S. known for complex topography, emissions, and meteorology that can result in periods of high wintertime levels[37, 38]. The PCAPS correlation to ambient measurements was better for $PM_{2.5}$ sulfate ion and elemental carbon than other reduced complexity tools and comparable to those same tools for $PM_{2.5}$ nitrate ion (Figure 5). PCAPS also compared similarly with the performance of other reduced complexity tools when considering fractional bias and fractional error metrics (Figure 5).

Model performance (Table 3) improved when the contribution of lateral boundary inflow was considered for $PM_{2.5}$ nitrate and sulfate even though this amount is fairly small at most monitors[21]. This contribution becomes more influential in more recent years as emissions decrease from U.S. anthropogenic sources and shows that reduced complexity tools that do not consider lateral boundary inflow should systematically underestimate observation data at some locations. The discrepancy was most notable for $PM_{2.5}$ sulfate performance for 2016, which has lower SO_2 emissions and $PM_{2.5}$ sulfate measurements at monitors compared to 2007 and 2011. Performance metrics improved with the addition of a contribution representing lateral boundary inflow.

LIMITATIONS & NEXT DIRECTION

The generic sources used to train PCAPS did not include everywhere in the U.S. which means some localized features important for transport or chemical transformation may not be well represented. The generic sources were each modeled for a single year which may not fully represent all meteorological conditions in a particular area important for O_3 or $PM_{2.5}$ formation. The generic sources tracked for contribution represent typical industrial facilities and surface level sectors emitting at ambient conditions (e.g., mobile sources). The source-receptor relationships provided in this assessment would not be expected to provide realistic impacts for large wildfires, offshore sources, oceanic emissions, biogenic emissions, lightning, or volcanos.

Areas where O_3 is often VOC limited and NO_X emissions destroy O_3 faster than it can be produced may not always be well characterized. The chemical mix of pollutants from the year modeled for these sources may not represent other years in the distant past or future where emissions might be substantially different resulting in different preferential regimes for O_3 or $PM_{2.5}$ formation. However, areas with strongly VOC limited chemistry for O_3 production may be better represented by this tool for more recent and future years as these areas become smaller[31]. This approach does not currently represent secondary organic aerosol formation from volatilized primary organic aerosol emissions, VOC partitioning to the particulate phase, or complex secondary organic aerosol enhancements related to the presence of NO_X, SO_2, or NH_3 emissions[32, 33, 39].

This reduced complexity tool would not have the capability to predict situations where the underlying photochemical grid model cannot capture certain complex processes that can lead to elevated $PM_{2.5}$ or O_3. These situations can happen in areas of complex terrain and emissions and can be associated with periods of intense wind stagnation, such as wintertime O_3 and $PM_{2.5}$ in areas of the western U.S. This tool is not intended to provide interactions between predicted O_3 and $PM_{2.5}$, such as increases in $PM_{2.5}$ resulting in lower O_3 predictions due to light attenuation or ammonia substitution that can happen from changing levels of NO_X and SO_2.

The PCAPS tool will be used to develop a new source-receptor matrix that relates emissions in specific counties to annual average $PM_{2.5}$ and seasonal average MDA8 O_3 impacts to each county in the contiguous U.S. These grid-to-grid source-receptor relationships will be estimated at the PCAPS 12 km grid scale then aggregated to county level for use in an upcoming version of the COBRA tool. The COBRA tool is publicly available and will be the mechanism for dissemination of the data and approach described in this assessment.

Supplementary Material

Refer to Web version on PubMed Central for supplementary material.

Acknowledgements

REFERENCES

1. U.S. Environmental Protection Agency, Integrated Science Assessment (ISA) for Particulate Matter (Final Report, DEc 2019). U.S. Environmental Protection Agency, Washington, DC, EPA/600/R-19/188, 2019. 2019.

2. U.S. Environmental Protection Agency, U.S. EPA. Integrated Science Assessment (ISA) for Ozone and Related Photochemical Oxidants (Final Report, Apr 2020). U.S. Environmental Protection Agency, Washington, DC, EPA/600/R-20/012, 2020. 2020.

3. U.S. Environmental Protection Agency, Supplement to the 2019 Integrated Science Assessmenet for Particulate Matter. EPA/600/R-22/028. www.epa.gov/isa. 2022.

4. Kelly JT; Koplitz SN; Baker KR; Holder AL; Pye HO; Murphy BN; Bash JO; Henderson BH; Possiel NC; Simon H, Assessing PM2. 5 model performance for the conterminous US with comparison to model performance statistics from 2007–2015. Atmospheric Environment 2019, 214, 116872.

5. Simon H; Baker KR; Phillips S, Compilation and interpretation of photochemical model performance statistics published between 2006 and 2012. Atmospheric Environment 2012, 61, 124–139.

6. Cao M; Xing J; Sahu SK; Duan L; Li J, Accurate prediction of air quality response to emissions for effective control policy design. Journal of Environmental Sciences 2023, 123, 116–126.

7. Mailloux NA; Abel DW; Holloway T; Patz JA, Nationwide and Regional PM2. 5-Related Air Quality Health Benefits From the Removal of Energy-Related Emissions in the United States. GeoHealth 2022, 6 (5), e2022GH000603.

8. Muller NZ; Mendelsohn R, The Air Pollution Emission Experiments and Policy Analysis Model (APEEP) Technical Appendix. J Yale University: New Haven, CT, USA. 2006.

9. Baker KR; Foley KM, A nonlinear regression model estimating single source concentrations of primary and secondarily formed PM2.5. Atmospheric Environment 2011, 45 (22), 3758–3767.

10. Heo J; Adams PJ; Gao HO, Reduced-form modeling of public health impacts of inorganic PM2. 5 and precursor emissions. Atmospheric Environment 2016, 137, 80–89.

11. Simon H; Baker K; Sellers J; Amend M; Penn S; Bankert J; Chan E; Fann N; Jang C; McKinley G, Evaluating reduced-form modeling tools for simulating ozone and PM2. 5 monetized health impacts. J Environmental Science: Atmospheres 2023.

12. Tessum CW; Hill JD; Marshall JD, InMAP: A model for air pollution interventions. PloS one 2017, 12 (4), e0176131. [PubMed: 28423049]

13. Van Dingenen R; Dentener F; Crippa M; Leitao J; Marmer E; Rao S; Solazzo E; Valentini L; Physics, TM5-FASST: a global atmospheric source–receptor model for rapid impact analysis of emission changes on air quality and short-lived climate pollutants. J Atmospheric Chemistry 2018, 18 (21), 16173–16211.

14. Henneman LR; Dedoussi IC; Casey JA; Choirat C; Barrett SR; Zigler CM, Comparisons of simple and complex methods for quantifying exposure to individual point source air pollution emissions. Journal of exposure science environmental epidemiology 2021, 31 (4), 654–663. [PubMed: 32203059]

15. Heo J; Adams PJ; Gao HO, Public health costs of primary PM2. 5 and inorganic PM2. 5 precursor emissions in the United States. Environmental Science & Technology 2016, 50 (11), 6061–6070. [PubMed: 27153150]

16. Skamarock WC; Klemp JB; Dudhia J; Gill DO; Barker DM; Duda MG; Huang X; Wang W; Powers JG, A description of the Advanced Reserch WRF version 3. NCAR Technical Note NCAR/TN-475+STR 2008.

17. U.S. Environmental Protection Agency, 2017 National Emission Inventory Technial Support Document. https://www.epa.gov/air-emissions-inventories/2017-national-emissions-inventory-nei-technical-support-document-tsd. 2020.

18. Solomon PA; Crumpler D; Flanagan JB; Jayanty R; Rickman EE; McDade CE, US national PM2. 5 chemical speciation monitoring networks—CSN and IMPROVE: description of networks. J Journal of the Air Waste Management Association 2014, 64 (12), 1410–1438.

19. U.S. Environmental Protection Agency, 2017 National Emission Inventory Based Photochemical Modeling for Source Sector Specific Air Quality Assessments. EPA-454/R-21–005. https://www.epa.gov/system/files/documents/2021-08/epa-454-r-21-005.pdf. 2021.

20. Yarwood G; Koo B, Final Report Improved OSAT, APCA and PSAT Algorithms for CAMx. Work Order No. 582-15-54388-011. Contract # 582-15-50417. Project 2015-45 task 4. Prepared under contract from the Texas Commission on Environmental Quality. 2015.

21. Baker KR; Emery C; Dolwick P; Yarwood G, Photochemical grid model estimates of lateral boundary contributions to ozone and particulate matter across the continental United States. Atmospheric Environment 2015, 123, 49–62.

22. Kwok R; Baker K; Napelenok S; Tonnesen G, Photochemical grid model implementation and application of VOC, NO x, and O 3 source apportionment. J Geoscientific Model Development Discussions 2015, 8 (1), 99–114.

23. Pay MT; Gangoiti G; Guevara M; Napelenok S; Querol X; Jorba O; Pérez García-Pando C, Ozone source apportionment during peak summer events over southwestern Europe. J Atmospheric chemistry physics 2019, 19 (8), 5467–5494.

24. Qi H; Duan W; Cheng S; Cai B, O3 transport characteristics in eastern China in 2017 and 2021 based on complex networks and WRF-CMAQ-ISAM. J Chemosphere 2023, 139258.

25. Shu Q; Napelenok SL; Hutzell WT; Baker KR; Murphy B; Hogrefe C; Henderson BH, Source Attribution of Ozone and Precursors in the Northeast US Using Multiple Photochemical Model Based Approaches (CMAQ v5. 3.2 and CAMx v7. 10). J Geoscientific Model Development Discussions 2022, 2022, 1–34.

26. Sulaymon ID; Zhang Y; Hopke PK; Ye F; Gong K; Mao J; Hu J, Modelling PM2. 5 during severe atmospheric pollution episode in Lagos, Nigeria: Spatiotemporal variations, source apportionment, and meteorological influences. J Journal of Geophysical Research: Atmospheres 2023, e2022JD038360.

27. Wang Q; Wang X; Huang R; Wu J; Xiao Y; Hu M; Fu Q; Duan Y; Chen J, Regional transport of PM2. 5 and O3 based on complex network method and chemical transport model in the Yangtze River Delta, China. J Journal of Geophysical Research: Atmospheres 2022, 127 (5), e2021JD034807.

28. Baker KR; Kelly JT, Single source impacts estimated with photochemical model source sensitivity and apportionment approaches. Atmospheric Environment 2014, 96, 266–274.

29. Baker KR; Woody MC, Assessing Model Characterization of Single Source Secondary Pollutant Impacts Using 2013 SENEX Field Study Measurements. Environmental Science & Technology 2017, 51 (7), 3833–3842. [PubMed: 28248097]

30. Baker KR; Kotchenruther RA; Hudman RC, Estimating ozone and secondary PM 2.5 impacts from hypothetical single source emissions in the central and eastern United States. Atmospheric Pollution Research 2016, 7 (1), 122–133.

31. Koplitz S; Simon H; Henderson B; Liljegren J; Tonnesen G; Whitehill A; Wells B, Changes in ozone Chemical Sensitivity in the United States from 2007 to 2016. ACS Environmental Au 2021.

32. Carlton AG; Pye HO; Baker KR; Hennigan CJ, Additional benefits of federal air-quality rules: Model estimates of controllable biogenic secondary organic aerosol. Environmental Science & Technology 2018, 52 (16), 9254–9265. [PubMed: 30005158]

33. Wagstrom KM; Baker KR; Leinbach AE; Hunt SW, Synthesizing scientific progress: Outcomes from US EPA's carbonaceous aerosols and source apportionment STAR grants. Environmental Science & Technology 2014, 48 (18), 10561–10570. [PubMed: 25111572]

34. Baker KR; Amend M; Penn S; Bankert J; Simon H; Chan E; Fann N; Zawacki M; Davidson K; Roman H, A database for evaluating the InMAP, APEEP, and EASIUR reduced complexity air-quality modeling tools. Data in Brief 2020, 28, 104886. [PubMed: 31872009]

35. Gilmore EA; Heo J; Muller NZ; Tessum CW; Hill JD; Marshall JD; Adams PJ, An inter-comparison of the social costs of air quality from reduced-complexity models. J Environmental Research Letters 2019, 14 (7), 074016.

36. Dolwick P; Akhtar F; Baker KR; Possiel N; Simon H; Tonnesen G, Comparison of background ozone estimates over the western United States based on two separate model methodologies. Atmospheric Environment 2015, 109, 282–296.

37. Kelly JT; Parworth CL; Zhang Q; Miller DJ; Sun K; Zondlo MA; Baker KR; Wisthaler A; Nowak JB; Pusede SE, Modeling NH4NO3 over the San Joaquin Valley during the 2013 DISCOVER-AQ campaign. Journal of Geophysical Research: Atmospheres 2018, 123 (9), 4727–4745.

38. Sun X; Ivey CE; Baker KR; Nenes A; Lareau NP; Holmes HA, Confronting Uncertainties of Simulated Air Pollution Concentrations during Persistent Cold Air Pool Events in the Salt Lake Valley, Utah. Environmental Science & Technology 2021, 55 (22), 15072–15081. [PubMed: 34709803]

39. Carlton AG; de Gouw J; Jimenez JL; Ambrose JL; Attwood AR; Brown S; Baker KR; Brock C; Cohen RC; Edgerton S, Synthesis of the southeast atmosphere studies: Investigating fundamental atmospheric chemistry questions. J Bulletin of the American Meteorological Society 2018, 99 (3), 547–567.

SYNOPSIS

A new reduced complexity model was developed to estimate annual average $PM_{2.5}$ and seasonal average O_3, which allows regulating agencies to quickly quantify impacts of emission control plans.
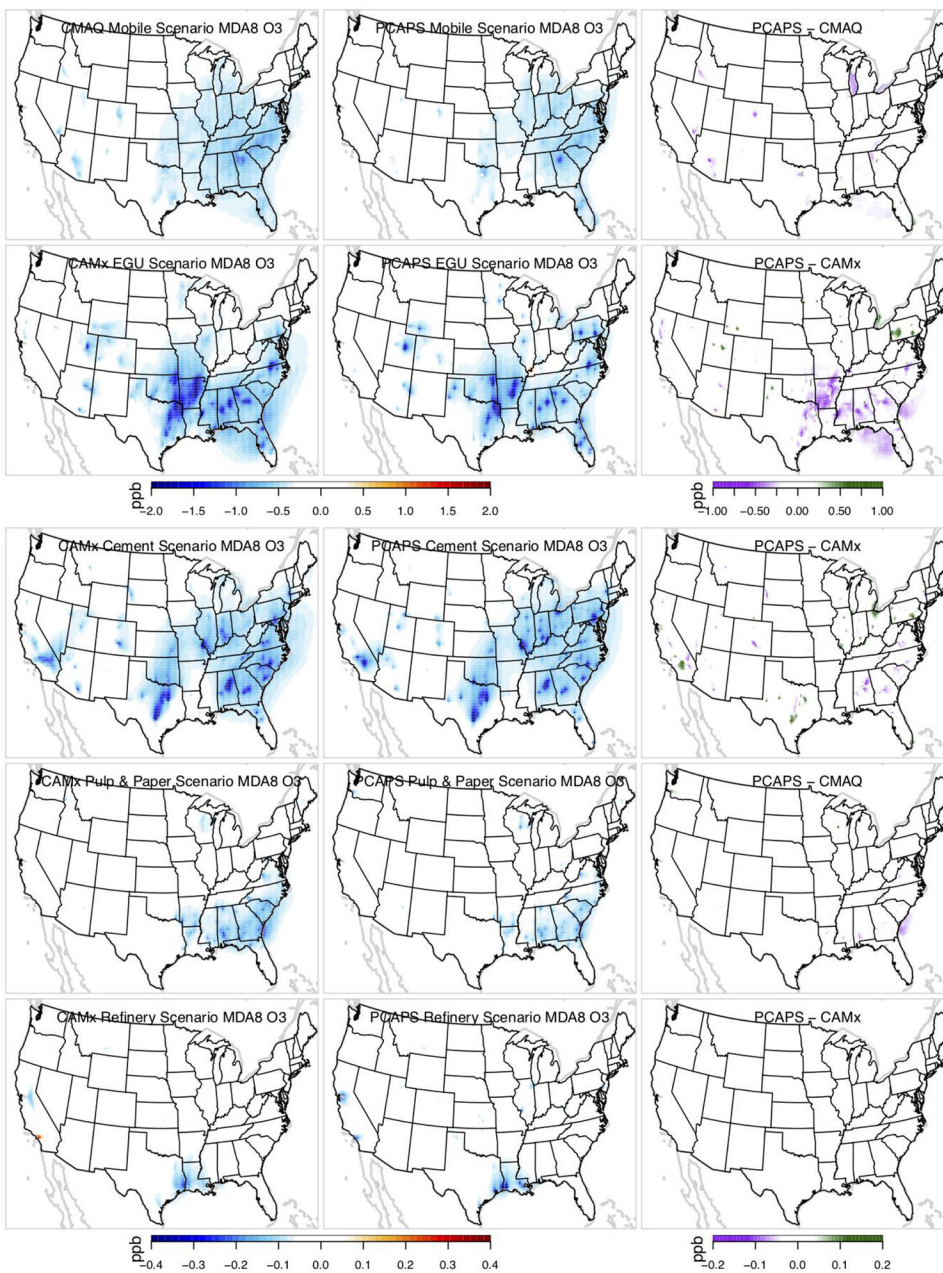
Figure 1.
Spatial representation of photochemical (left panels) and PCAPS (center panels) model prediction of change in seasonal average MDA8 O$_3$ for each of the emission scenarios. The difference between predicted change in air quality between these models is also shown (right panels).

Figure 2.
Spatial representation of photochemical (left panels) and PCAPS (center panels) model prediction of change in annual average PM$_{2.5}$ for each of the emission scenarios. The difference between predicted change in air quality between these models is also shown (right panels).
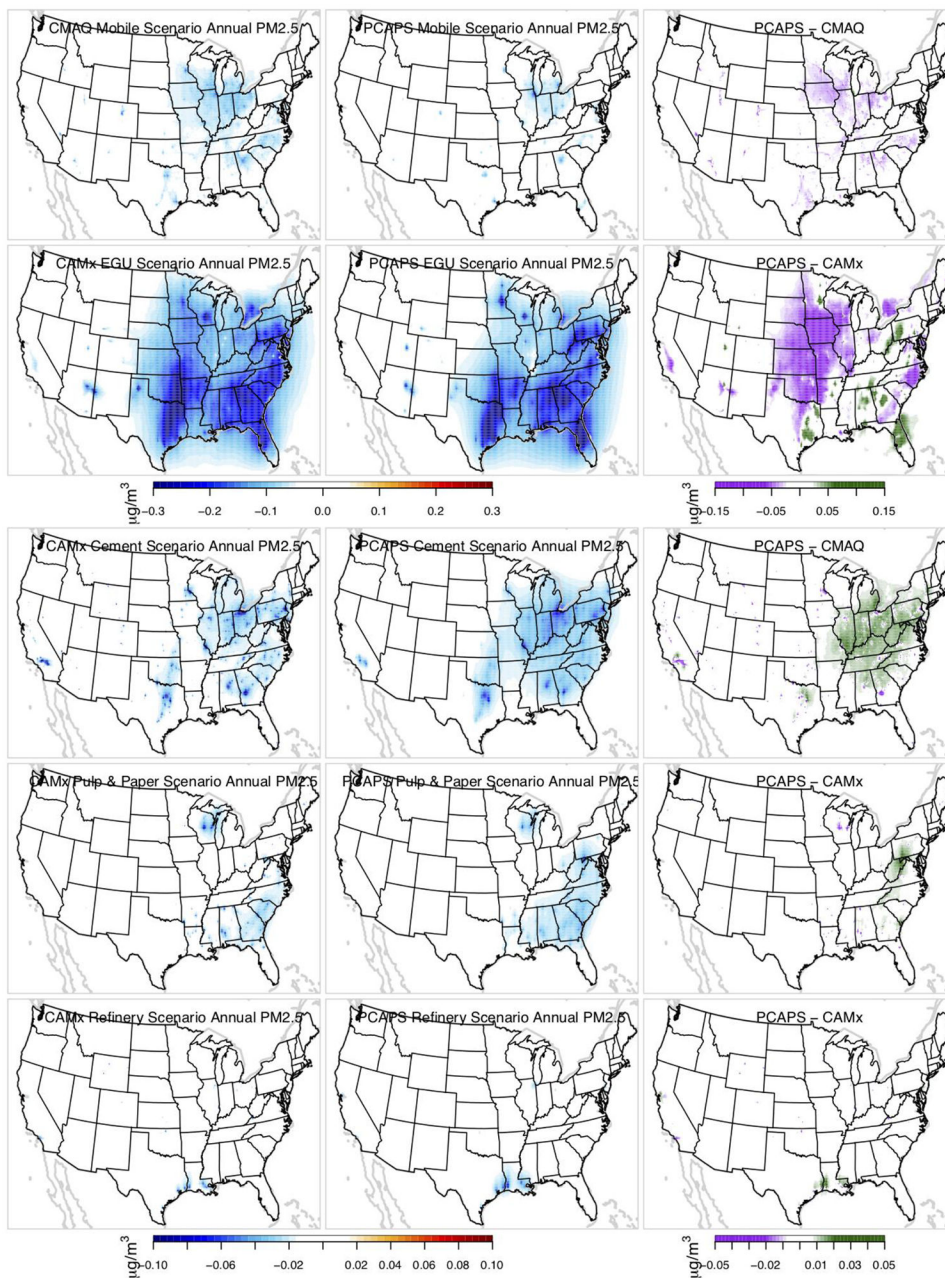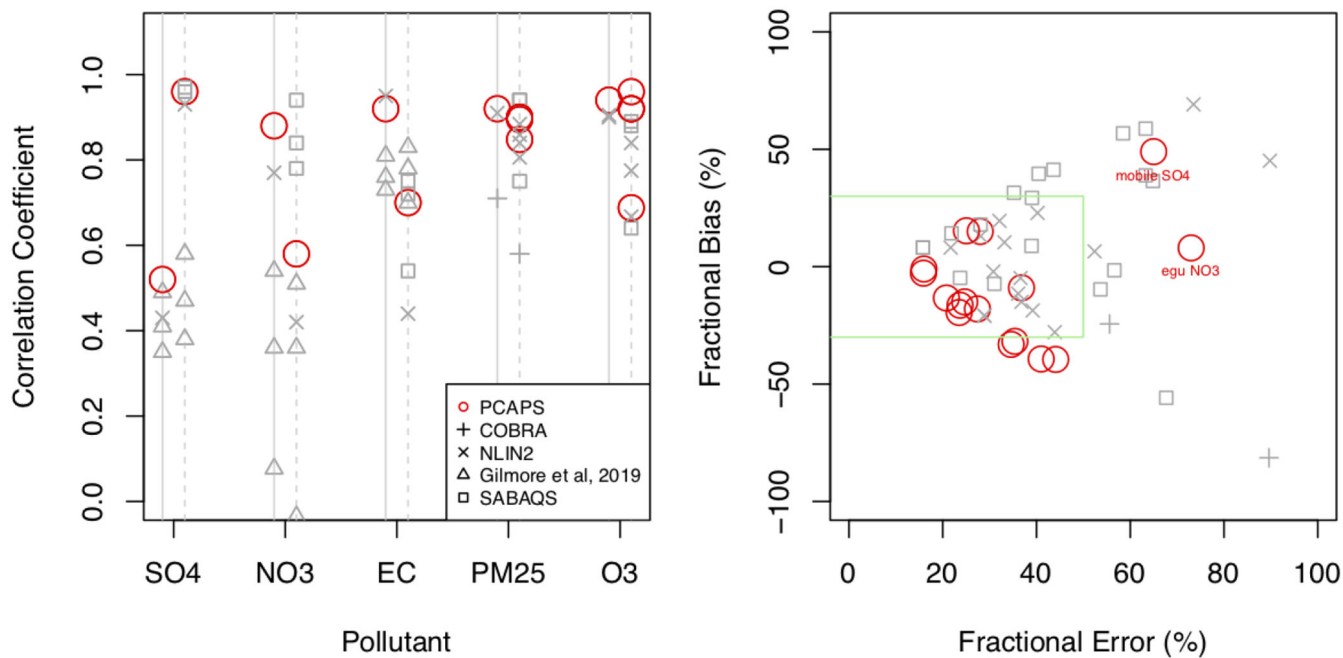
Figure 3.
Performance metrics comparing PCAPS, NLIN2, COBRA, and SABAQS with photochemical grid model predictions for multiple emission control scenarios. Similar metrics are shown from Gilmore et al, 2019 comparing model predicted PM$_{2.5}$ components between multiple reduced complexity models for an emission scenario representing all U.S. emissions in 2005. The solid trace on the left panel shows performance metrics for surface level (solid trace) and elevated emissions (dashed trace) scenarios.
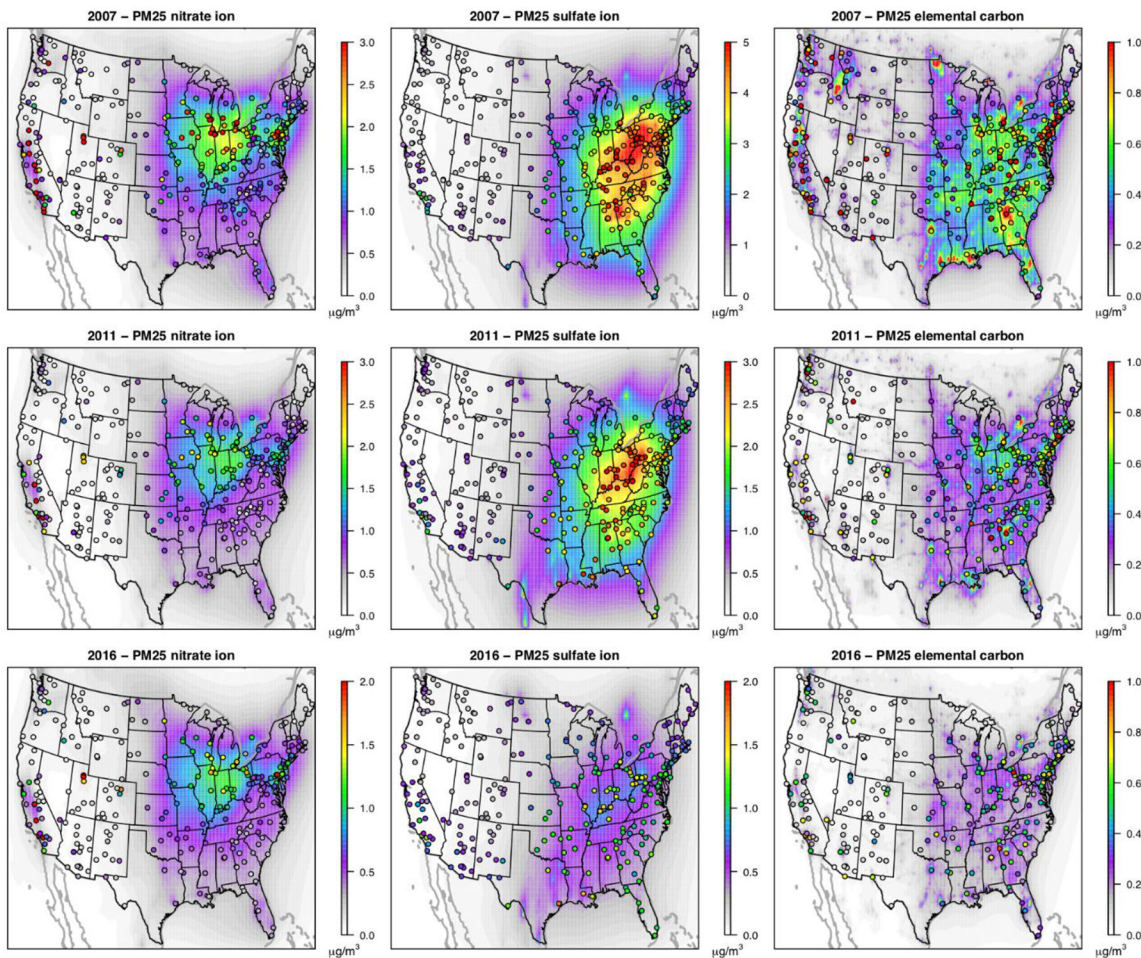
Figure 4.

Annual average PCAPS predicted PM$_{2.5}$ sulfate ion, PM$_{2.5}$ nitrate ion, and PM$_{2.5}$ elemental carbon with annual average ambient measurements from routine surface level networks. A comparison is shown for 2007, 2011, and 2016 using emissions and ambient data from those years.

Figure 5.
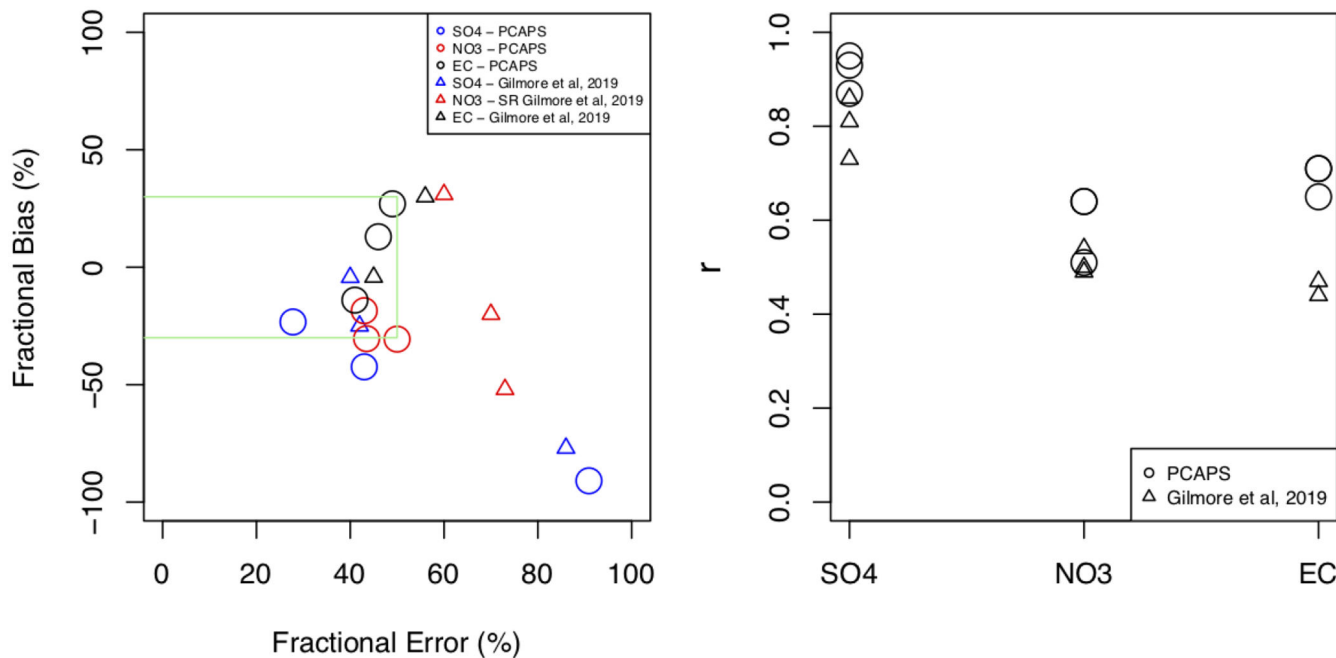Performance metrics for three different years calculated without lateral boundary inflow contribution comparing model predicted $PM_{2.5}$ sulfate ion, $PM_{2.5}$ nitrate ion, and $PM_{2.5}$ elemental carbon with routine surface monitoring sites. Metrics are shown for PCAPS and other reduced complexity tools assessed in Gilmore et al, 2019.

Table 1.

Performance metrics comparing PCAPS with photochemical model (CMAQ) predicted change in seasonal MDA8 O_3 with two complex emission control scenarios for each grid cell in multiple regions and the entire U.S. Modeled means and mean bias (MB) expressed in ppb. Normalized mean bias (NMB), fractional bias (FB), and fractional error (FE) expressed as a percent.

| Seasonal O3 | Mobile Control Scenario | | | | | | | EGU Control Scenario | | | | | | |
| | SRM | CMAQ | | | | | | SRM | CAMx | | | | | |
Region	mean	mean	MB	NMB	FB	FE	r	mean	mean	MB	NMB	FB	FE	r
Northeast	−0.31	−0.27	−0.04	15.4	14.3	18.3	0.93	−0.31	−0.26	−0.04	16.66	15.4	22.5	0.77
Northern Rockies	−0.11	−0.13	0.03	−18.9	−20.9	21.1	0.94	−0.15	−0.16	0.01	−5.44	−5.6	13.6	0.92
Northwest	−0.09	−0.12	0.03	−26.6	−30.7	38.9	0.70	−0.03	−0.05	0.02	−31.68	−37.6	43.9	0.93
Ohio Valley	−0.48	−0.48	0.00	0.6	0.6	11.3	0.49	−0.35	−0.42	0.07	−15.83	−17.2	22.9	0.82
South	−0.26	−0.31	0.05	−15.3	−16.5	20.5	0.88	−0.47	−0.58	0.11	−18.21	−20.0	24.3	0.93
Southeast	−0.58	−0.58	0.00	−0.7	−0.7	11.1	0.80	−0.56	−0.70	0.14	−19.93	−22.1	26.7	0.85
Southwest	−0.15	−0.21	0.06	−27.6	−32.1	33.1	0.81	−0.24	−0.27	0.03	−11.40	−12.1	19.1	0.88
Upper Midwest	−0.26	−0.27	0.01	−3.9	−4.0	13.8	0.82	−0.25	−0.27	0.03	−10.02	−10.6	19.8	0.51
West	−0.06	−0.07	0.02	−21.5	−24.1	30.6	0.94	−0.07	−0.12	0.05	−39.06	−48.5	53.1	0.47
US	−0.25	−0.27	0.02	−8.7	−9.1	18.1	0.94	−0.29	−0.34	0.05	−15.16	−16.4	23.7	0.92

Table 2.

Performance metrics comparing PCAPS with photochemical model predicted change in annual average $PM_{2.5}$ with two complex emissions control scenarios for each grid cell in multiple regions and the entire U.S. Modeled means and mean bias (MB) expressed in $\mu g/m^3$. Normalized mean bias (NMB), fractional bias (FB), and fractional error (FE) expressed as a percent.

Annual PM2.5	Mobile Control Scenario							EGU Control Scenario						
	SRM	CMAQ						SRM	CAMx					
Region	mean	mean	MB	NMB	FB	FE	r	mean	mean	MB	NMB	FB	FE	r
Northeast	−0.022	−0.023	0.001	−2.5	−2.5	20.5	0.89	−0.096	−0.102	0.005	−5.4	−5.5	18.2	0.93
Northern	−0.006	−0.011	0.005	−48.6	−64.3	65.5	0.96	−0.021	−0.035	0.015	−41.4	−52.2	57.0	0.92
Northwest	−0.004	−0.007	0.003	−45.9	−59.6	73.7	0.65	−0.002	−0.004	0.001	−37.0	−45.4	54.8	0.50
Ohio Valley	−0.045	−0.062	0.018	−28.8	−33.6	35.0	0.85	−0.125	−0.144	0.018	−12.8	−13.7	22.2	0.66
South	−0.016	−0.029	0.013	−43.7	−55.9	56.5	0.91	−0.123	−0.144	0.021	−14.7	−15.8	21.4	0.90
Southeast	−0.035	−0.045	0.010	−21.8	−24.4	35.3	0.70	−0.203	−0.200	−0.003	1.6	1.6	16.1	0.77
Southwest	−0.005	−0.009	0.003	−40.2	−50.3	57.3	0.81	−0.027	−0.032	0.004	−13.3	−14.3	26.1	0.85
Upper Midwest	−0.032	−0.050	0.018	−36.5	−44.6	45.9	0.86	−0.081	−0.117	0.036	−30.9	−36.6	41.6	0.53
West	−0.001	−0.002	0.001	−39.7	−49.6	57.9	0.75	−0.005	−0.009	0.004	−48.0	−63.2	67.5	0.77
US	−0.017	−0.026	0.008	−33.0	−39.5	44.1	0.92	−0.076	−0.088	0.012	−13.9	−15.0	24.7	0.90

Table 3.

PCAPS prediction of $PM_{2.5}$ nitrate ion, $PM_{2.5}$ sulfate ion, and $PM_{2.5}$ elemental carbon using emissions from the 2007, 2011, and 2016 National Emission Inventories compared with annual average speciated $PM_{2.5}$ measurements made at routine surface monitor networks. Metrics for $PM_{2.5}$ sulfate and nitrate were calculated with and without contribution from the lateral boundary inflow (BCON) estimated by a photochemical grid model. The mean bias (MB) is expressed in $\mu g/m^3$. Normalized mean bias (NMB), fractional bias (FB), and fractional error (FE) expressed as a percent.

Specie	Year	N	MB	NMB	FB	FE	r	BCON
PM2.5 elemental carbon	2007	344	0.17	31.8	27.4	49.2	0.65	N
PM2.5 elemental carbon	2011	311	0.06	13.5	12.6	45.5	0.71	N
PM2.5 elemental carbon	2016	280	−0.04	−12.9	−13.7	41.2	0.71	N
PM2.5 nitrate ion	2007	344	−0.33	−26.5	−30.6	50.0	0.51	N
PM2.5 nitrate ion	2011	311	−0.14	−16.9	−18.5	43.2	0.64	N
PM2.5 nitrate ion	2016	280	−0.16	−26.4	−30.4	43.5	0.64	N
PM2.5 sulfate ion	2007	344	−0.51	−20.9	−23.3	27.8	0.95	N
PM2.5 sulfate ion	2011	311	−0.54	−35.0	−42.4	43.0	0.93	N
PM2.5 sulfate ion	2016	280	−0.51	−62.5	−90.9	90.9	0.87	N
PM2.5 nitrate ion	2007	344	−0.22	−17.7	−19.4	46.0	0.53	Y
PM2.5 nitrate ion	2011	311	−0.03	−3.9	−4.0	40.3	0.66	Y
PM2.5 nitrate ion	2016	280	−0.05	−8.7	−9.1	38.4	0.66	Y
PM2.5 sulfate ion	2007	344	0.04	1.6	1.5	14.4	0.96	Y
PM2.5 sulfate ion	2011	311	0.01	0.4	0.4	15.0	0.94	Y
PM2.5 sulfate ion	2016	280	0.05	5.9	5.7	22.3	0.91	Y